Australia's Wine Future

A CLIMATE ATLAS

Remenyi, T.A. [1,2]; Rollins, D.A. [1,2]; Love, P.T. [1,2]; Earl, N.O. [1,2]; Bindoff, N.L. [1,3]; Harris, R.M.B. [1,2]

[1] Climate Futures, Antarctic Climate & Ecosystems CRC, University of Tasmania, Hobart
[2] Discipline of Geography & Spacial Sciences, University of Tasmania, Hobart
[3] Institute for Marine and Antarctic Studies (IMAS), University of Tasmania, Hobart

This research was funded by the Wine Australia Project UT1504
'Australia's Wine Future: Adapting to short-term climate variability and long-term climate change'

Contact: Rebecca.Harris@utas.edu.au

Disclaimer

The material in this atlas is based on computer modelling projections for climate change scenarios and, as such, there are inherent uncertainties in the data. While every effort has been made to ensure the material in this atlas is accurate, Wine Australia and the University of Tasmania provide no warranty, guarantee or representation that the material will prove to be accurate, complete, up-to-date, non-infringing or fit for purpose. The use of the material is entirely at the risk of the user. The user must independently verify the suitability of the material for their own use.

To the maximum extent permitted by law, Wine Australia and the University of Tasmania, any other participating organisation and their officers, employees, contractors and agents exclude liability for any loss, damage, costs or expenses whether direct, indirect, consequential including loss of profits, opportunity and third party claims that may be caused through the use of, reliance upon, or interpretation of the material in this atlas.

Citation

Remenyi, T.A., Rollins, D.A., Love, P.T., Earl, N.O., Bindoff, N.L., Harris, R.M.B. (2019) *Australia's Wine Future — A Climate Atlas*, University of Tasmania, Hobart, Tasmania.

ISBN: 978-1-922352-06-4 (electronic); 978-1-922352-05-7 (print)

Acknowledgements

The authors would like to acknowledge Wine Australia and the Antarctic Climate & Ecosystems CRC (University of Tasmania) for their funding and support.

Our CSIRO colleagues, Dr Marcus Thatcher, Dr Tony Rafter, Dr Claire Trenham and Dr Matt Paget produced the underlying data and collaborated in the validation and analysis of the climate trends.

Our UTas, SARDI and AWRI colleagues, Dr Fiona Kerslake, Dr Peter Hayman, Dr Dane Thomas, Dr Paul Petrie and Dr Mark Kristic provided valuable connections, perspectives and insights into the wine industry. Their involvement enabled us to understand the true needs of growers and wine makers.

Many industry contributors hosted us during visits and generously gave us their time in interviews. Their constructive feedback was invaluable in making sure that the atlas is relevant and accessible.

This project used the R programming language and would therefore like to recognise the efforts of the *R-core team* and those of *RStudio* in providing the tools and interfaces that made data analysis and visualisation possible and innovative. This project also used the LaTeXtypesetting system. We would like to recognise the contributors to this system.

A special thanks to Dr Michael Sumner for all his efforts upskilling our team in programming, workflow management, geospatial data and a host of specific programming packages we used within this project.

Requests and enquiries

Requests and enquiries concerning reproduction rights should be addressed to:

Communications and Media Office
University of Tasmania
+61 3 6226 2124
Media.Office@utas.edu.au

AUSTRALIA'S WINE FUTURE
A CLIMATE ATLAS

BAROSSA VALLEY

RAINFALL

Projected Mean Growing Season Rainfall

1997–2017	2041–2060	2081–2100
220 mm	225 mm	209 mm

TEMPERATURE

Projected Mean Growing Season Temperature

1997–2017	2041–2060	2081–2100
19.0 °C	20.3 °C	21.8 °C

EXTREME HEAT

Projected Mean Excess Heat Factor

1997–2017	2041–2060	2081–2100
20.0 EHF	22.0 EHF	23.7 EHF

EXTREME COLD

Projected Mean Growing Season Frost Risk Days

1997–2017	2041–2060	2081–2100
0.9 days	0.2 days	0.0 days

ARIDITY

Projected Mean Annual Aridity Index

1997–2017	2041–2060	2081–2100
0.33	0.26	0.21

Wine Australia

ACE CRC ANTARCTIC CLIMATE & ECOSYSTEMS COOPERATIVE RESEARCH CENTRE

climatefutures

UNIVERSITY of TASMANIA

BAROSSA VALLEY

Heat

Figure 1: Observed mean Growing Season Temperature

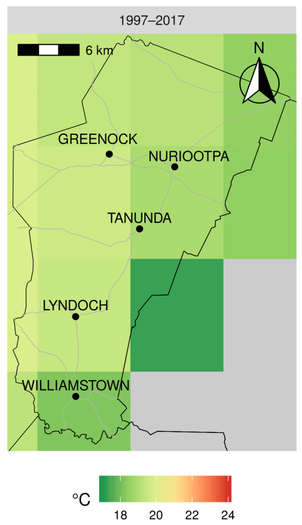

Figure 2: Observed change in mean Growing Season Temperature

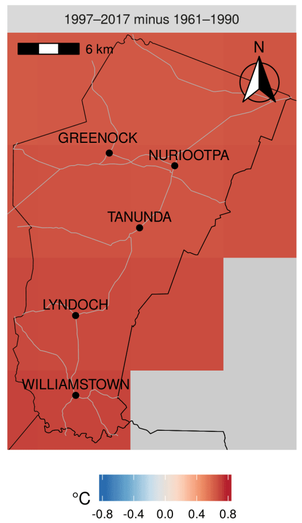

Figure 3: Projected mean Growing Season Temperature

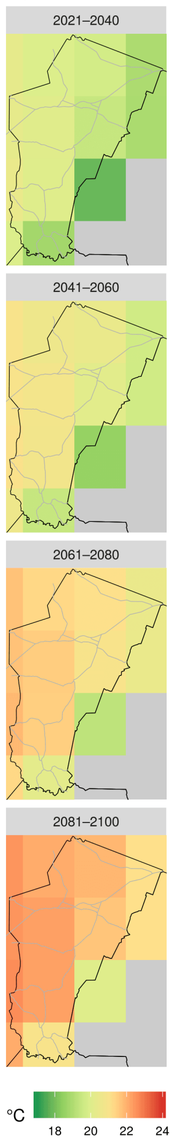

Figure 1: Observed mean *Growing Season Temperature* (Oct–Apr) across all growing years from 1997–2017.

Figure 2: The change in *Growing Season Temperature* between the current (1997–2017) and historical (1961–1990) periods. *Growing Season Temperature* has increased across the region over recent decades.

Figure 3: Projected mean *Growing Season Temperature* (Oct–Apr) for 20-year time periods from 2021 to 2100. *Growing Season Temperature* is expected to increase steadily into the future. Each grid cell is the mean of the 6 ensemble members.

Figure 4: Projected Growing Season Temperature (October to April)

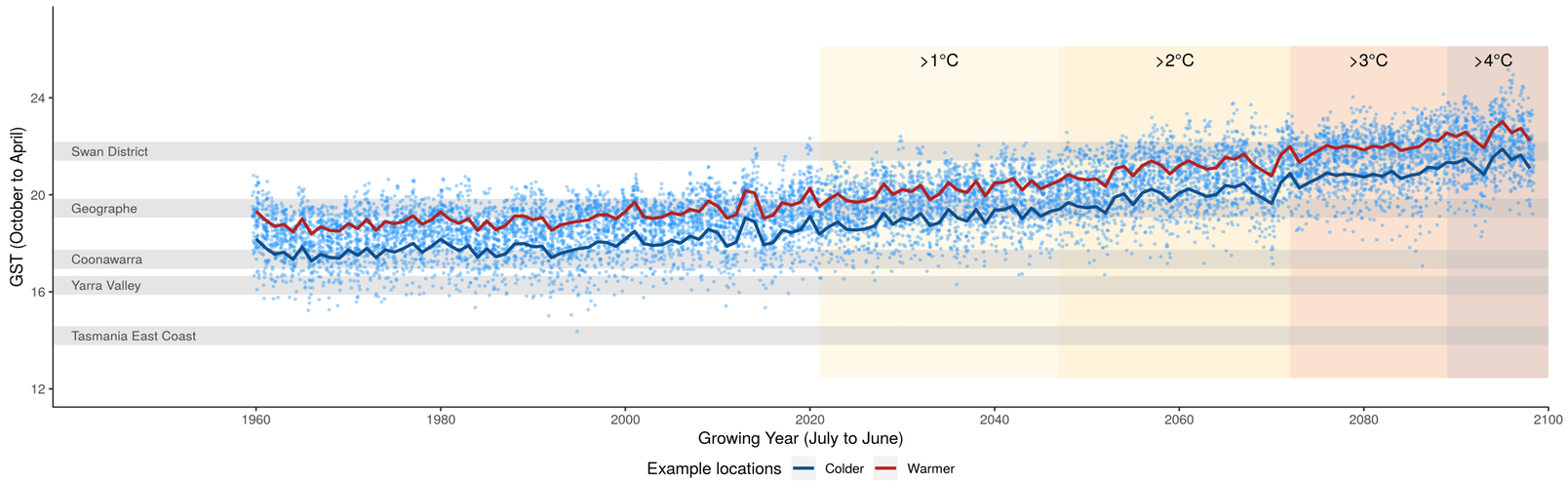

Figure 4: *Growing Season Temperature* (GST) over time. Blue points are the values for each grid cell, for each of the 6 ensemble members. Solid lines are timeseries representing grid cells for colder and warmer locations within the region based on current conditions (1997–2017). Horizontal grey bars represent the mean GST value during 1997–2017 in selected regions across Australia. These provide a comparison between current conditions elsewhere and future conditions in this region, helping to identify future analogue regions. Coloured bars represent the projected global temperature increase expected into the future (following the RCP 8.5 scenario). These can be used to make decisions based on *projected temperature change* rather than time (for example, if the rate of warming rapidly increases, useful information can still be extracted from these figures by using the shade boxes instead of the time-axis).

Figure 5: Distribution of Growing Season Temperature

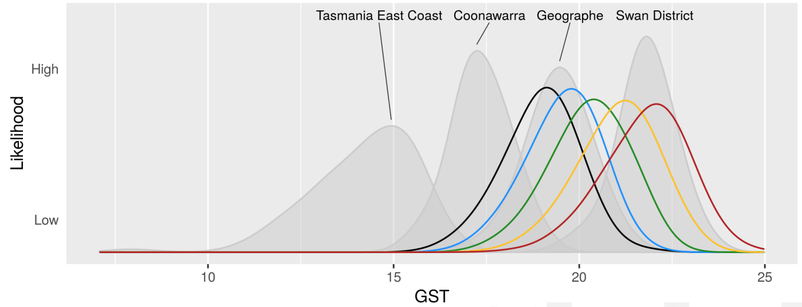

Figure 5: Probability distribution of GST for 20-year time periods from 2001 to 2100. Variability can occur spatially within the region, across years, or between ensemble members. Grey shapes represent the probability distribution of GST for contrasting regions during 1997–2017. A shift to the right (left) indicates warmer (cooler) conditions.

Figure 6: Distribution of Growing Degree Days

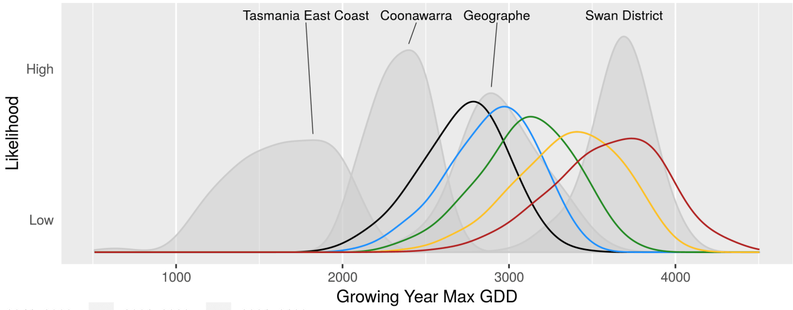

Figure 6: Probability distribution of growing year maximum GDD for 20-year time periods from 2001 to 2100. Variability can occur spatially within the region, across years, or between ensemble members. Grey shapes represent the probability distribution of growing year maximum GDD for contrasting regions during 1997–2017. A shift to the right (left) indicates warmer (cooler) conditions.

Figure 7: Projected cumulative Growing Degree Days

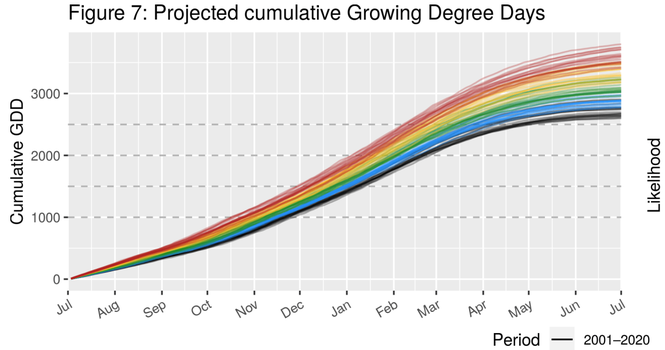

Figure 7: Cumulative *Growing Degree Days* (GDD) across the growing year (July–June). Dashed lines show GDD values (1000, 1500, 2000, 2500) for some example phenological thresholds. Each growing year is represented by a coloured line. In future time periods, heat accumulates faster, thresholds are reached earlier and maximum GDD reached is higher.

Figure 8: Distribution of date when Growing Degree Days reaches threshold

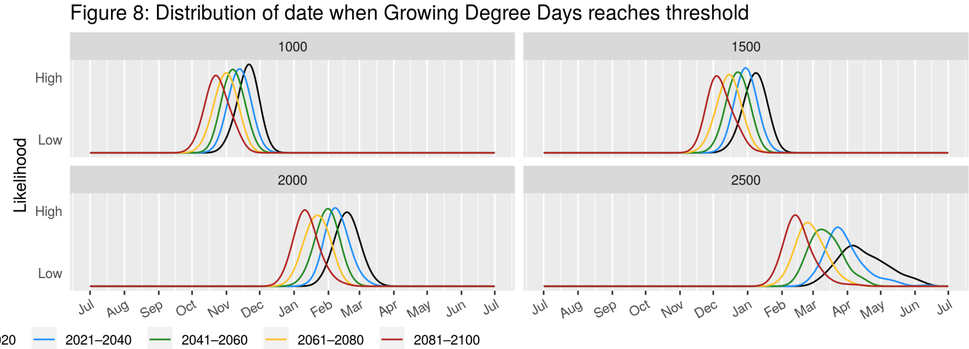

Figure 8: Probability distributions showing the range of dates at which the example phenological thresholds (1000, 1500, 2000, 2500) are reached for each time period. Variability can occur spatially within the region, across years, or between ensemble members. A shift to the left (right) indicates earlier (later) harvest dates. A wider (thinner) curve indicates a larger (smaller) range of harvest dates. A missing time period indicates that the specific phenological threshold was not reached within the growing year (July–June).

BAROSSA VALLEY

Moisture

Figure 1: Observed mean Growing Season Rainfall

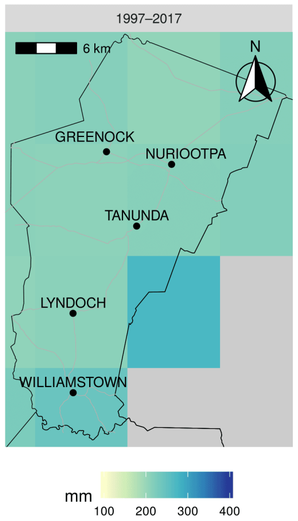

Figure 2: Observed change in mean Growing Season Rainfall

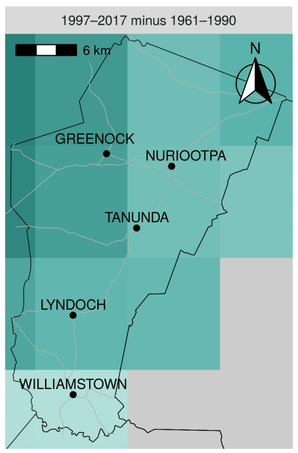

Figure 3: Projected mean Growing Season Rainfall

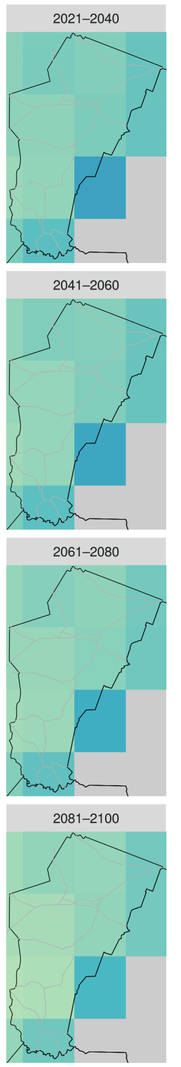

Figure 1: Observed mean *Growing Season Rainfall* (Oct–Apr) across all growing years from 1997–2017.

Figure 2: Change in *Growing Season Rainfall* (Oct–Apr) between the current (1997–2017) and historical (1961–1990) periods. Negative values indicate a trend towards drier conditions. Positive values indicate a trend towards wetter conditions.

Figure 3: Projected mean *Growing Season Rainfall* (Oct–Apr) for 20-year time periods from 2021 to 2100. Each grid cell is the mean of the 6 ensemble members.

Figure 4: Projected Growing Season Rainfall (October to April)

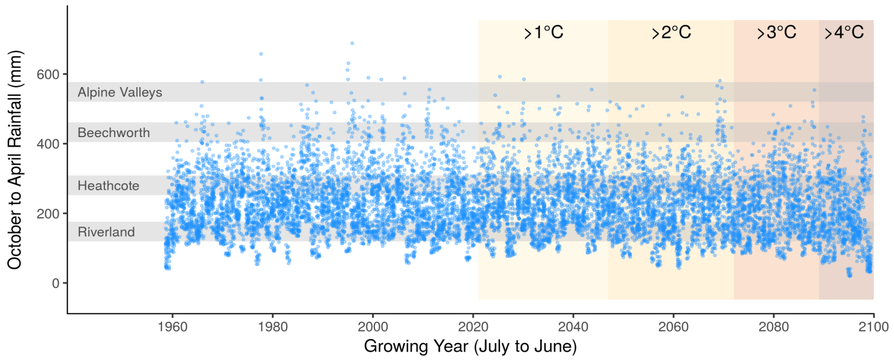

Figure 5: Projected Non-Growing Season Rainfall (May to September)

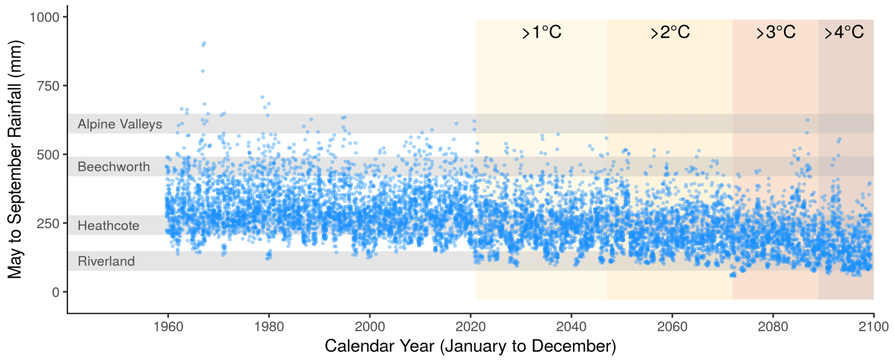

Figure 4: Time series of *Growing Season Rainfall* (mm). Blue points are the annual values for each grid cell, for each of the 6 ensemble members. Horizontal grey bars represent the mean *Growing Season Rainfall* value during 1997–2017 in selected regions across Australia. These provide a comparison between current conditions (1997–2017) elsewhere and future conditions in this region and help identify future analogue regions. Coloured bars represent the projected mean global temperature increase into the future (following the RCP 8.5 scenario). These can be used to make decisions based on *projected temperature change* rather than time.

Figure 5: As with Figure 4, but for *Non-Growing Season Rainfall* (mm). Horizontal grey bars represent the mean *Non-Growing Season Rainfall* value during 1997–2017 in selected regions across Australia.

Figure 6: Projected monthly rainfall

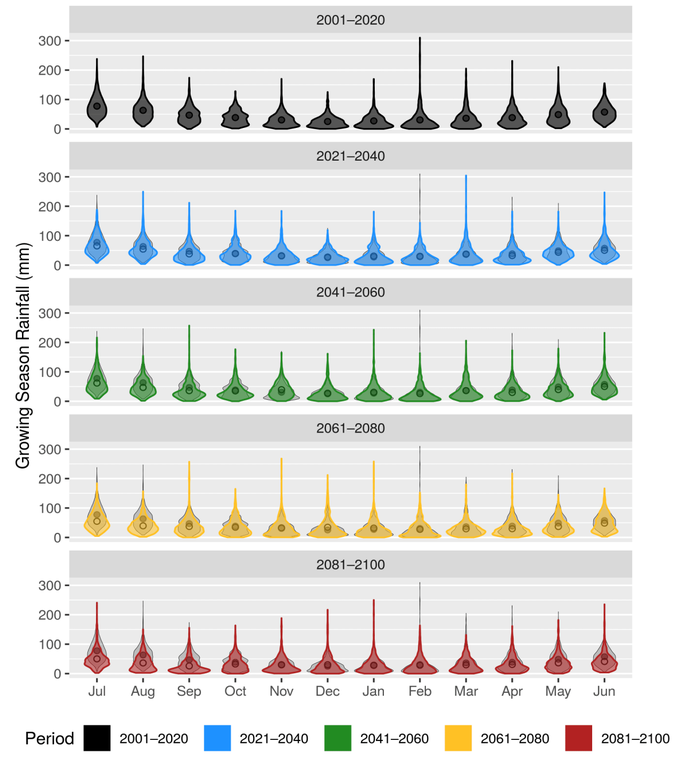

Figure 6: *Violin plots* of monthly rainfall (mm) for 20-year time periods from 2001 to 2100. Each violin represents monthly totals for each grid cell, for each of the 6 ensemble members, and for each growing year within the time period. In each panel the monthly violins indicate the expected probability distribution of rainfall across the growing year. The current period (2001–2020) is shadowed underneath the future time periods to highlight any differences expected into the future. Dots represent the mean monthly rainfall for each violin. If the violin shifts lower (higher) this indicates a change towards drier (wetter) conditions.

Figure 7: Distribution of seasonal rainfall

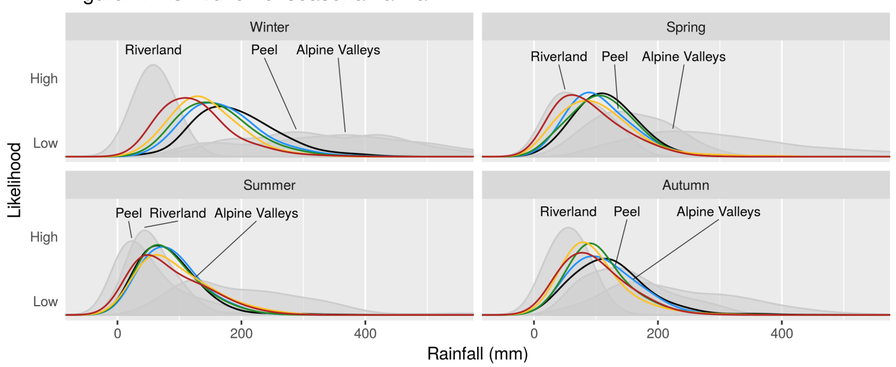

Figure 8: Distribution of number of rainy days during harvest

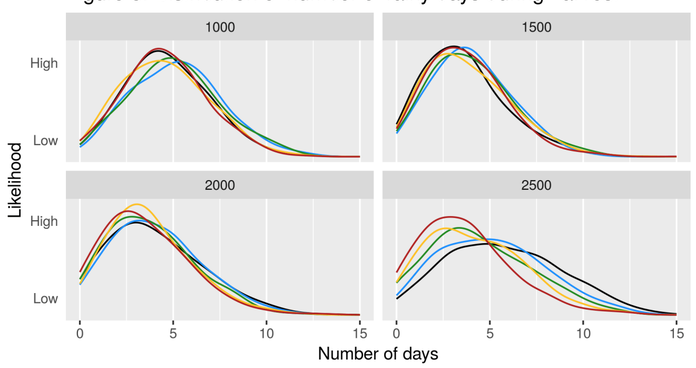

Figure 7: Seasonal rainfall (Winter, Spring, Summer, Autumn) (mm), presented as a probability distribution for each 20-year period. The shape of the curve is driven by the level of variability experienced within each 20-year period. Variability can occur spatially within the region, across years, or between ensemble members. Grey shapes represent the probability distribution of seasonal rainfall for contrasting regions during 1997–2017. Differences in the shape of curves between the current and future periods indicate a change in the typical conditions. A shift to the left (right) indicates an increase in drier (wetter) conditions.

Figure 8: Number of rainy days during harvest for each 20-year period. *Harvest* refers to the date when *Growing Degree Days* (GDD) reach example phenological thresholds (1000, 1500, 2000, 2500) which were chosen to reflect development time of different grape styles and varieties. Rainy days during harvest were defined as days with >10mm of rain from 7 days before to 7 days after the date each GDD threshold was reached. Variability can occur spatially within the region, across years, or between ensemble members. A shift in the curve to the left (right) indicates fewer (more) rainy days during harvest. A missing time period indicates that the specific phenological threshold was not reached within the growing year (July–June).

BAROSSA VALLEY

Aridity

Figure 1: Observed mean annual Aridity Index

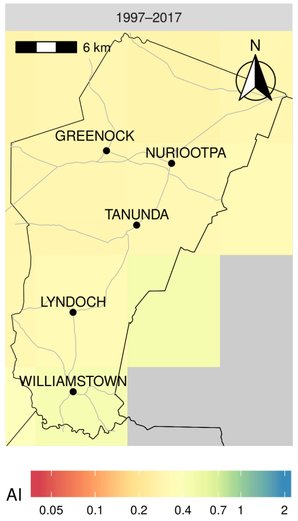

Figure 2: Obseved change in mean annual Aridity Index

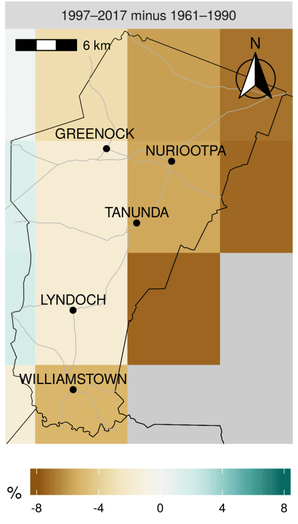

Figure 3: Projected mean annual Aridity Index

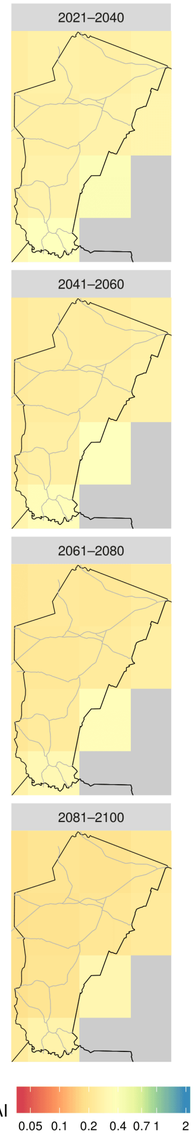

Figure 1: Observed mean annual Aridity Index across all growing years from 1997–2017. Aridity Index is a value that characterises the ratio between the mean annual rainfall and mean annual evaporation. Low (high) values indicate drier (wetter) conditions.

Figure 2: Observed percentage change in mean annual Aridity Index between the current (1997–2017) and historical (1961–1990) periods. This shows the change already experienced across the region. Negative (positive) values indicate a trend towards drier (wetter) conditions.

Figure 3: Projected mean annual Aridity Index for 20-year time periods from 2021 to 2100. Each grid cell is the mean of the 6 ensemble members. Decreasing (increasing) values indicate a trend towards drier (wetter) conditions.

Figure 4: Projected Aridity Index

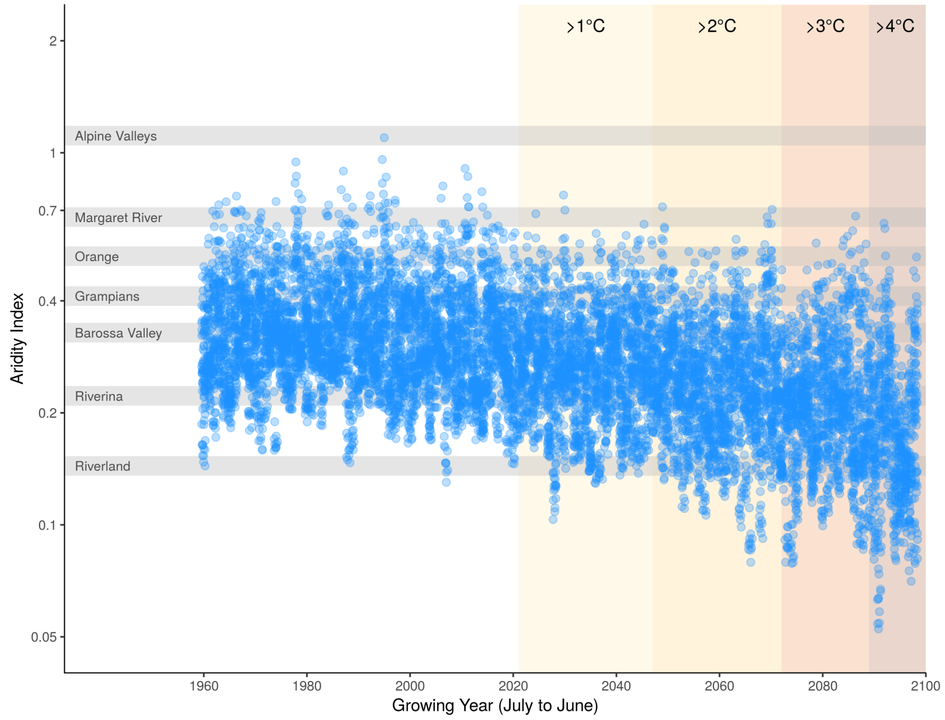

Figure 4: Time series of annual Aridity Index. Points are the annual means for each grid cell in the region, for each of the 6 ensemble members. Aridity Index values >2 all indicate very wet conditions. There is no meaningful difference past this value, so higher values were not presented. Horizontal grey bars represent the mean annual Aridity Index from selected regions across Australia — these provide an example of conditions this region may transition towards in the future. Coloured bars represent the projected global temperature increase expected in the future (following the RCP 8.5 scenario) which can be used to make decisions based on *projected temperature change* rather than *time* (for example, if the rate of warming rapidly increases, where temperature changes are experienced earlier, useful information can still be extracted from these figures by using the coloured boxes instead of the time-axis).

Figure 5: Projected monthly Aridity Index

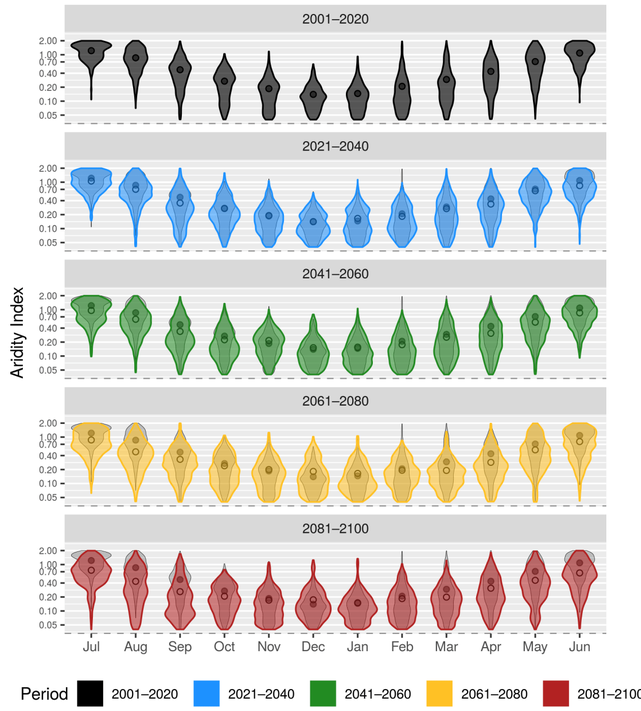

Figure 5: *Violin plots* of monthly Aridity Index for 20-year time periods from 2001 to 2100. Each violin represents monthly averages for each grid cell, for each of the 6 ensemble members, and for each growing year within the time period. In each 20-year panel the violins indicate the expected probability distribution of Aridity Index within each month across the growing year. The current period (2001–2020) is shadowed underneath the future time periods to highlight any differences expected into the future. Dots represent the mean monthly Aridity Index for each violin. If the violin shifts lower (higher) this indicates a change towards drier (wetter) conditions.

Figure 6: Distribution of seasonal Aridity Index

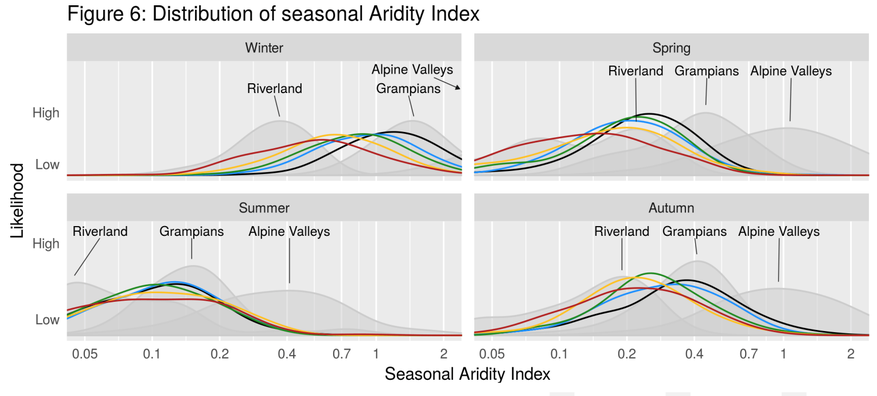

Figure 6: Seasonal Aridity Index (Winter, Spring, Summer, Autumn), presented as a probability distribution for each 20-year period. The shape of the curve is driven by the level of variability experienced within each 20-year period. Variability can occur spatially within the region, across years, or between ensemble members. Grey shapes represent the probability distribution of seasonal aridity for contrasting regions during 1997–2017. Differences in the shape of curves between the current and future periods indicate a change in the typical conditions. A shift to the left (right) indicates an increase in drier (wetter) conditions. Aridity Index values >2 all indicate very wet conditions.

Figure 7: Distribution of mean Aridity Index from July until harvest

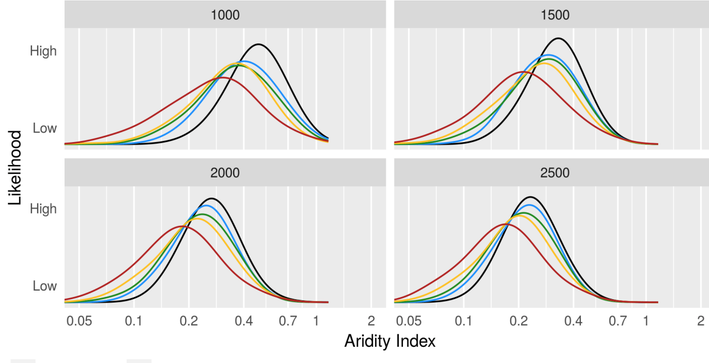

Figure 7: Mean annual Aridity Index accumulated from start of the growing season (July) to *date of harvest*, presented as a probability distribution for each 20-year period. *Date of harvest* refers to the date at which *Growing Degree Days* reach some example phenological thresholds (1000, 1500, 2000, 2500), chosen to reflect development time of different grape styles and varieties. Variability can occur spatially within the region, across years, or between ensemble members. A shift to the left (right) indicates drier (wetter) conditions. A missing time period indicates that the specific phenological threshold was not reached within the growing year (July–June).

BAROSSA VALLEY

Extremes — Hot

Figure 1: Observed mean Excess Heat Factor

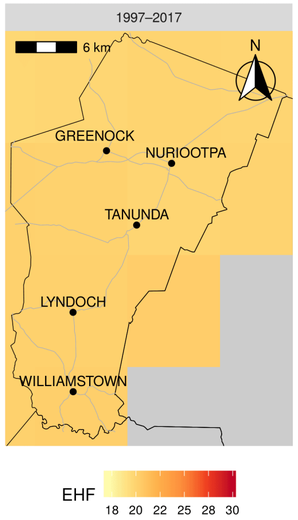

Figure 2: Observed change in mean Excess Heat Factor

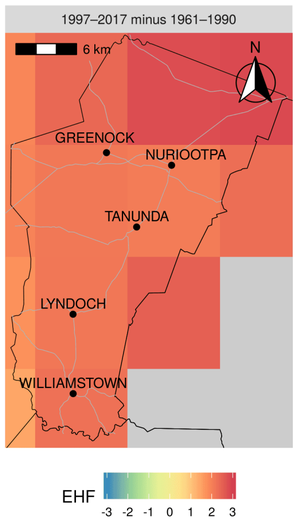

Figure 3: Projected mean Excess Heat Factor

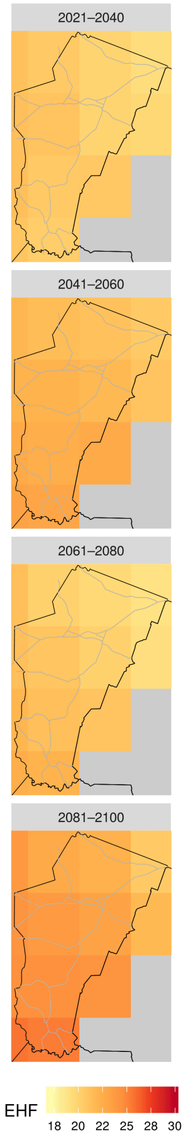

Figure 4: Projected mean number of extreme heat days

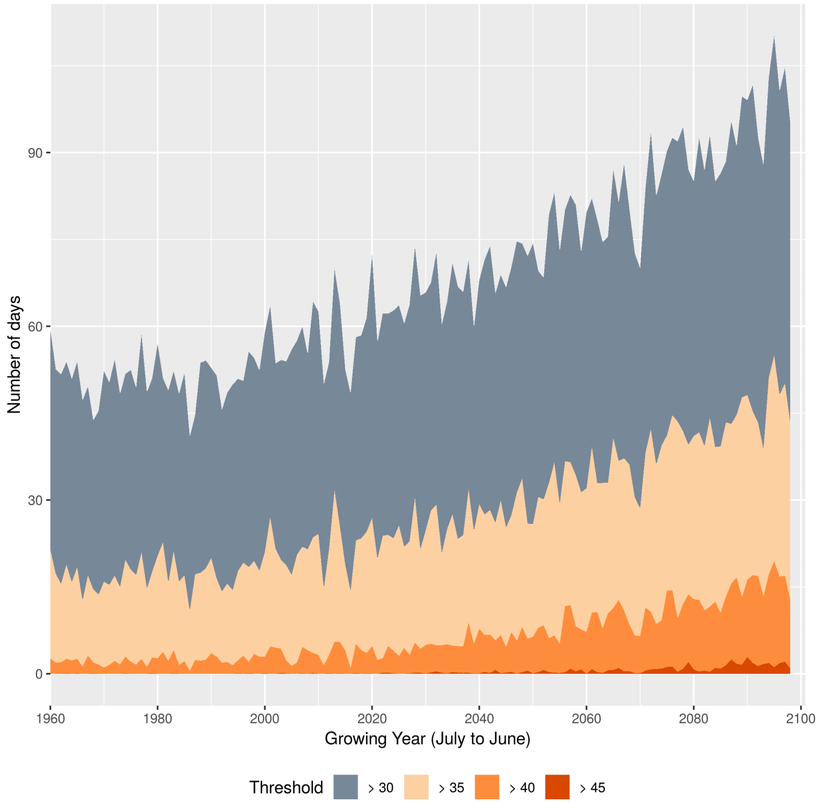

Figure 5: Projected number of days with severe risk to humans working outside

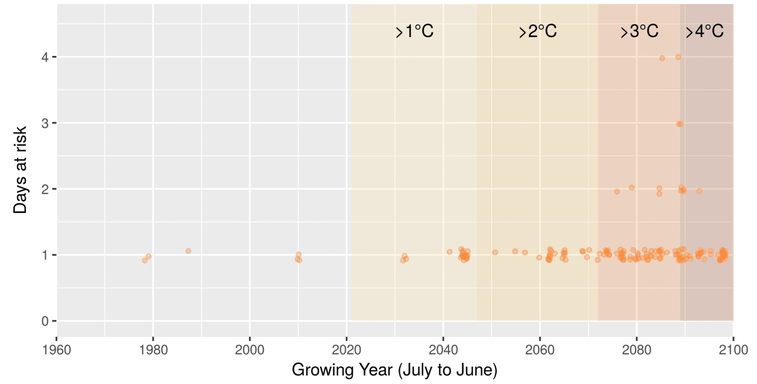

Figure 6: Projected range of hot summer days

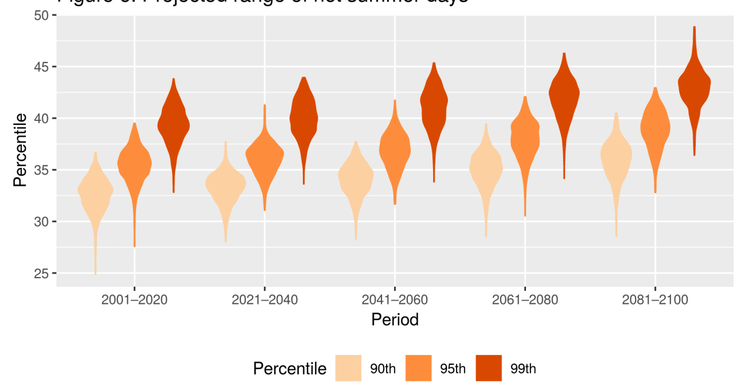

Figure 1: Observed mean *excess heat factor* (EHF) during heatwaves (as per Nairn and Fawcett (2013)), across all growing years from 1997–2017. EHF is an index that characterises heatwaves, high values indicate more intense heatwaves. The mean EHF is the mean value from all heatwaves that occurred from 1997–2017.

Figure 2: Change in mean EHF during heatwaves between the current (1997–2017) and historical (1961–1990) periods. Positive (negative) values indicate a trend towards more (less) intense heatwaves.

Figure 3: Projected mean EHF during heatwaves for 20-year time periods from 2021 to 2100. Each grid cell is the mean of the 6 ensemble members. Increasing (decreasing) values indicate a trend towards more (less) intense heatwaves.

Figure 4: Time series of the number of days per growing year with temperatures greater than 30°C, 35°C, 40°C and 45°C. Areas indicate the number of days each threshold is exceeded per growing year. Values are averaged across all grid cells and the 6 ensemble members. Colours indicate each of the extreme threshold values. Generally increasing frequencies reflect a warming climate.

Figure 5: Time series of the number of days per growing year of *High human heat stress*. This is defined as days when daily maximum temperatures are >30°C and daily minimum humidity is >60%. These conditions cause severe risk of heat stress to humans (and potentially low productivity) to those working in exposed areas. Humans cannot work in high temperature, high humidity environments without appropriate adaptive behaviours and equipment. Points are for each grid cell from each of the 6 ensemble members. Coloured bars represent the projected global temperature increase expected into the future (following the RCP 8.5 scenario) which can be used to make decisions based on *projected temperature change* rather than *time*.

Figure 6: *Violins plots* of high temperatures (°C) per growing year for 20-year time periods from 2001 to 2100. Colours indicate extreme threshold values (90th, 95th and 99th percentile) of temperature during each growing year. The 99th percentile value reflects the 4th hottest day each growing year; the 95th percentile is the 18th hottest day each growing year; and the 90th percentile is the 36th hottest day each growing 1year. Generally increasing values reflect a warming climate.

Figure 7: Distribution of daily minimum and maximum temperature during a heatwave

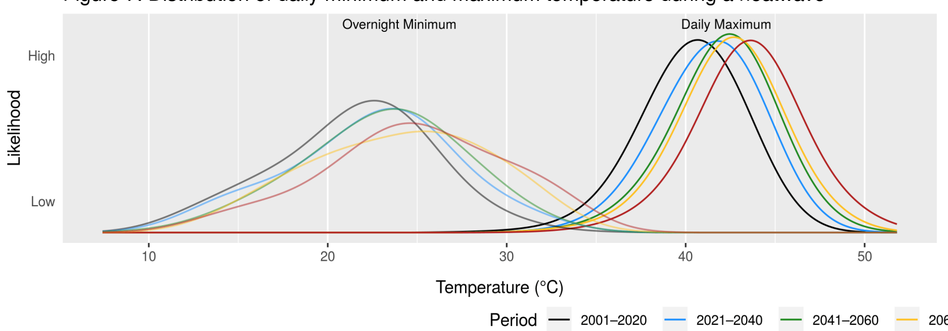

Figure 8: Distribution of date of heatwave days

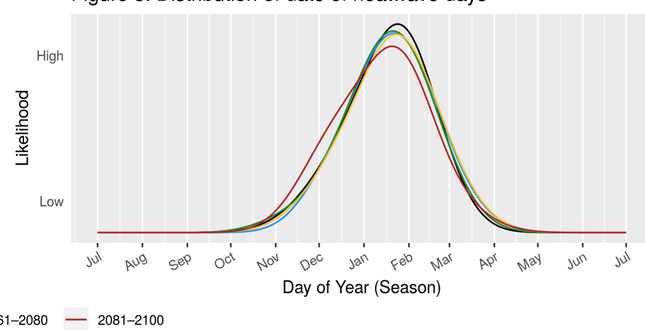

Figure 7: Probability distributions of daily maximum temperatures and minimum overnight temperatures during heatwaves. Colour of each curve indicates different 20-year periods. The shape of the curve is driven by the level of variability experienced within each 20-year period. Variability can occur spatially within the region, across years, or between ensemble members. A shift to the right (left) indicates higher (lower) temperature heatwaves.

Figure 8: Probability distribution of the date when heatwaves occur. The shape of the curve is driven by the level of variability experienced within each 20-year period. Variability can occur spatially within the region, across years, or between ensemble members. A shift to the left (right) indicates heatwaves occurring earlier (later).

BAROSSA VALLEY

Extremes — Cold

Figure 1: Observed mean frost risk days

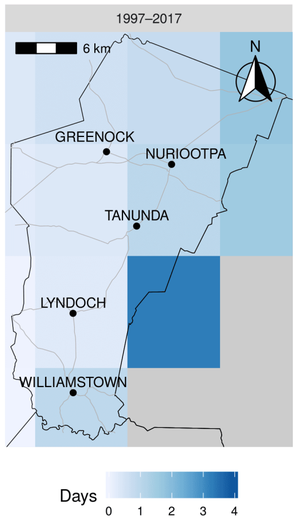

Figure 2: Observed change in mean frost risk days

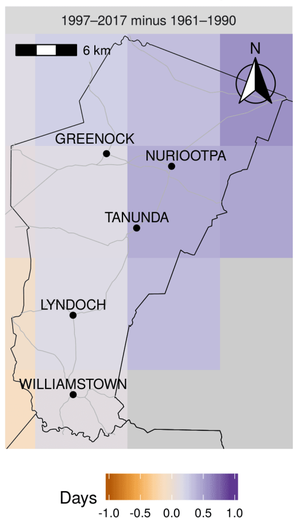

Figure 3: Projected mean frost risk days

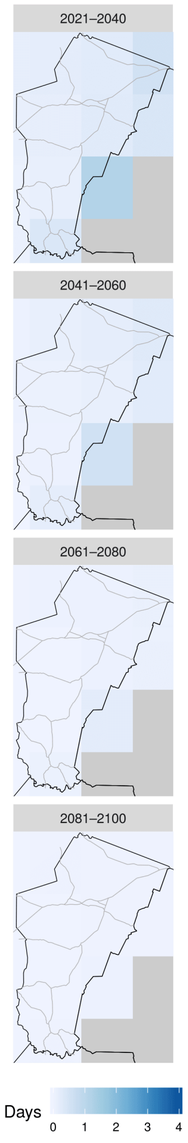

Figure 1: Observed mean number of days at risk of frost during the growing season (October to April) over the period 1997–2017. Days at risk of frost are those with a daily minimum temperature <2°C. High (low) values indicate high (low) frost risk.

Figure 2: Change in the mean number of days at risk of frost during the growing season (October to April) between the current (1997–2017) and historical (1961–1990) periods. Days at risk of frost are days with a minimum temperature <2°C. High (low) values indicate increased (decreased) frost risk.

Figure 3: Projected mean number of days at risk of frost during the growing season (October to April) for 20-year time periods from 2021 to 2100. Each grid cell is the mean of the 6 ensemble members. Increasing (decreasing) values indicate a trend towards higher (lower) frost risk.

Figure 4: Projected monthly minimum temperature

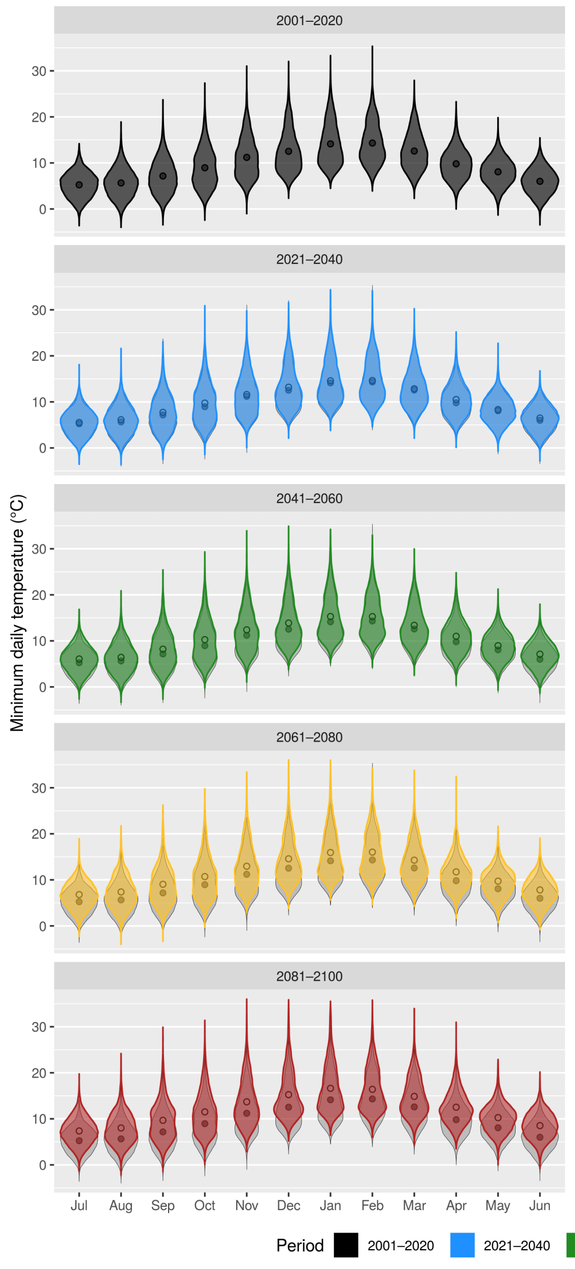

Figure 4: *Violin plots* of daily minimum temperature (°C) for each month for 20-year periods from 2001 to 2100. Each violin represents daily data for each grid cell, for each of the 6 ensemble members, and for each growing year within the time period; e.g. the top-left most violin represents the daily minimum temperature for every January day in the period 2001–2020, for each grid cell in the region, for each of the 6 ensemble members. The current period (2001-2020) has been shadowed underneath future time periods to highlight any differences expected into the future. Dots represent the means for each violin. If the violin shifts lower (higher) this indicates a change towards colder (warmer) conditions.

Figure 5: Projected monthly frost risk days

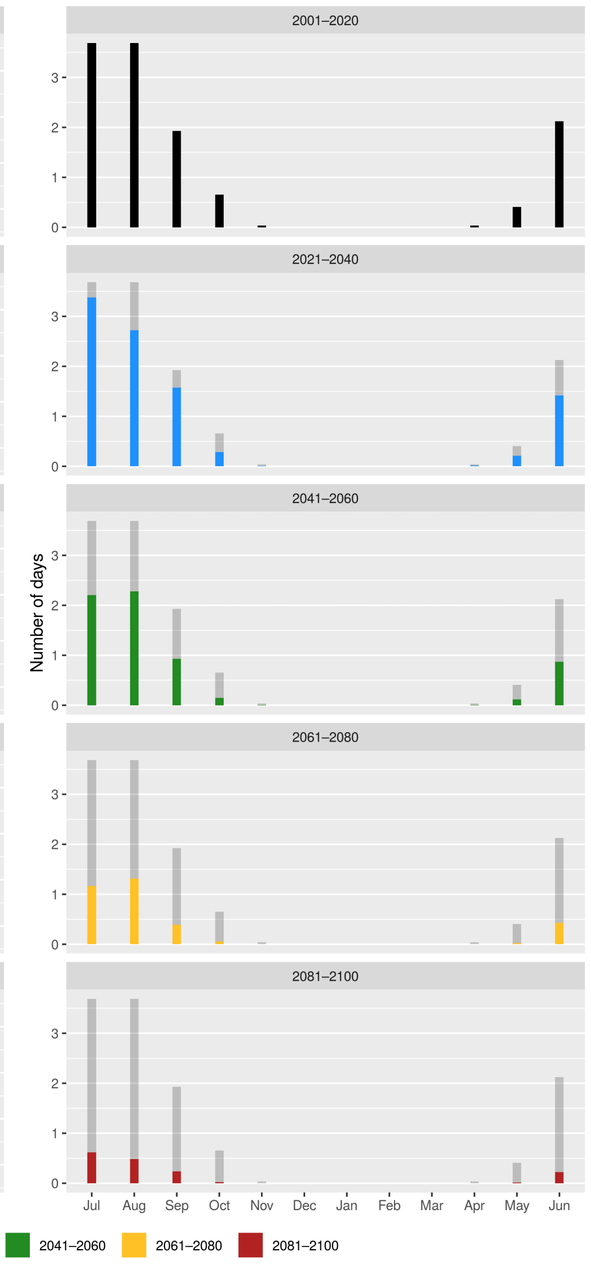

Figure 5: Monthly average cumulative frost days for 20-year periods from 2001 to 2100. Values are a summary across all grid cells, for all years with each 20-year period, for each of the 6 ensemble members. This reflects how frost risk varies across the year within each 20-year period. The current period (2001–2020) has been shadowed underneath future time periods to highlight any differences expected into the future.

Figure 6: Projected accumulated frost intensity

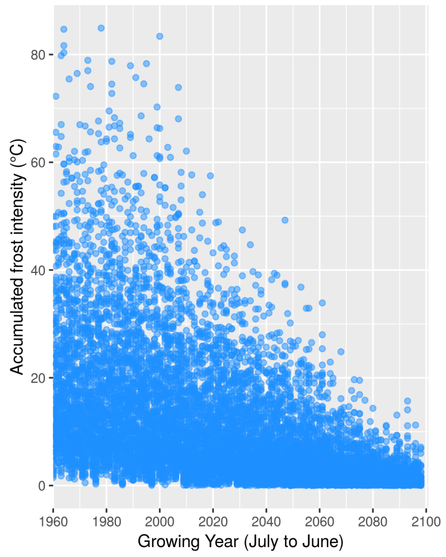

Figure 7: Projected mean number of extreme cold days

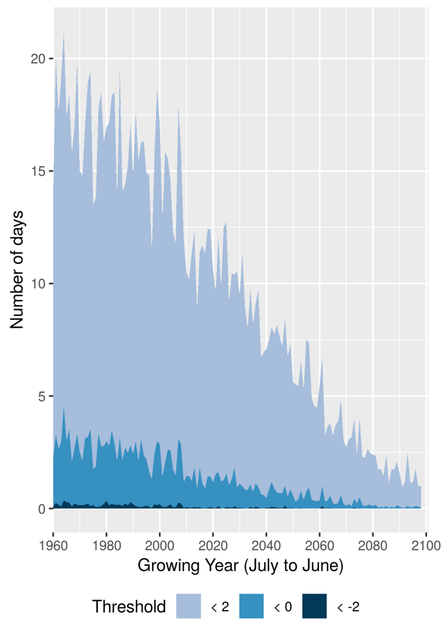

Figure 6: Timeseries of accumulated frost intensity, which is the cumulative total of temperatures less than 2°C over a growing season. This index characterises exposure to cold conditions. High values indicate cold winters/springs. Points are for each grid cell, averaged across the 6 ensemble members.

Figure 7: Time series of the number of days per growing year when temperature falls below selected thresholds (<2°C, <0°C, <-2°C). Areas indicate the number of days temperatures fall below each threshold per growing year. Values are averaged across all grid cells and the 6 ensemble members. Fewer instances reflect a warming climate.